

Modeling of transdermal drug delivery with a microneedle array

Y-G Lv^{1,2}, J Liu¹, Y-H Gao¹ and B Xu³

¹ Technical Institute of Physics and Chemistry, Chinese Academy of Sciences, Beijing 100080, People's Republic of China

² Graduate School of the Chinese Academy of Sciences, Beijing 100039, People's Republic of China

³ School of NanoSciences and NanoEngineering, State University of New York at Albany, NY 12203, USA

E-mail: jliu@cl.cryo.ac.cn

Received 8 June 2006, in final form 31 August 2006

Published 10 October 2006

Online at stacks.iop.org/JMM/16/2492

Abstract

Transdermal drug delivery is generally limited by the extraordinary barrier properties of the stratum corneum, the outer 10–15 μm layer of skin. A conventional needle inserted across this barrier and into deeper tissues could effectively deliver drugs. However, it would lead to infection and cause pain, thereby reducing patient compliance. In order to administer a frequent injection of insulin and other therapeutic agents more efficiently, integrated arrays with very short microneedles were recently proposed as very good candidates for painless injection or extraction. A variety of microneedle designs have thus been made available by employing the fabrication tools of the microelectronics industry and using materials such as silicon, metals, polymers and glass with feature sizes ranging from sub-micron to nanometers. At the same time, experiments were also made to test the capability of the microneedles to inject drugs into tissues. However, due to the difficulty encountered in measurement, a detailed understanding of the spatial and transient drug delivery process still remains unclear up to now. To better grasp the mechanisms involved, quantitative theoretical models were developed in this paper to simultaneously characterize the flow and drug transport, and numerical solutions were performed to predict the kinetics of dispersed drugs injected into the skin from a microneedle array. Calculations indicated that increasing the initial injection velocity and accelerating the blood circulation in skin tissue with high porosity are helpful to enhance the transdermal drug delivery. This study provides the first quantitative simulation of fluid injection through a microneedle array and drug species transport inside the skin. The modeling strategy can also possibly be extended to deal with a wider range of clinical issues such as targeted nanoparticle delivery for therapeutics or molecular imaging.

(Some figures in this article are in colour only in the electronic version)

Nomenclature

A_0	Specific area per unit volume of skin tissue (m^2)	D_1	Diffusion coefficient in drug solution ($\text{m}^2 \text{s}^{-1}$)
A_f	Surface occupied by drug solution (m^2)	D_2	Drug diffusion coefficient in skin tissue ($\text{m}^2 \text{s}^{-1}$)
A_s	Whole surface area (m^2)	D'	Hydraulic diameter (m)
C_1	Drug concentration in drug solution (units ml^{-1})	d_{needle}	Diameter of microneedle tip (m)
C_2	Drug concentration in skin tissue (units ml^{-1})	g	Drug consumed per volume and time by skin tissue (unit $\text{m}^{-3} \text{s}^{-1}$)

L	Length of considered tissue (m)
M	Weight of insulin per unit (kg/unit)
n	Number of needles in the array
Nu	Nusselt number
q	Flow rate of drug solution
r	Radius of microneedle tip (m)
Re	Reynolds number
S	Surface area of microneedle array (m ²)
s_t	Cross section tip area of a single microneedle (m ²)
Sh	Sherwood number
t	Time (s)
u	Velocity of drug solution (m s ⁻¹)
u_0	Initial effective injection velocity of drug solution (m s ⁻¹)
u_{int}	Velocity of moving interface (m s ⁻¹)
u_t	Injection velocity of a single microneedle (m s ⁻¹)
x	Coordinate (m)
x_0	Position of microneedle tip (m)
x_{int}	Position of moving interface (m)
$x_{int,max}$	Maximal saturating distance (m)
Δp	Pressure drop along the microneedle (Pa)

Greek symbols

α	Drug solution absorption rate per unit tissue volume (m ³ drug solution/m ³ tissues)
β	Absorption coefficient (m ³ drug solution/m ³ tissues/s)
ρ	Density of drug solution (kg m ⁻³)
ε_s	Areal porosity
ε_v	Volumetric porosity
ε	Average porosity
μ	Viscosity of drug solution (Pa s)
φ	Partition coefficient of the drug in skin tissue

1. Introduction

Effectively delivering drugs into the target tissues or organs of the human body has been a big challenge in medical science [1, 2]. With the development of many modern sophisticated drugs, demands for an appropriate method were placed at an extremely high level never encountered before. Typical routes for drug delivery generally rely on hypodermic needles and orally administered pills. Although they are quite effective in delivering drugs, insertion of such a needle is painful and may make sustained delivery difficult. Drugs taken orally often suffer from poor absorption and enzymatic degradation in the intestine and liver. Moreover, conventional techniques based on pills and injections are often not suitable for new therapeutic compounds produced by advanced biotechnology based on protein and DNA [3, 4]. Drug delivery across the skin using a patch is more appealing to the patient and offers the possibility of a controlled release over time [5, 6]. However, transdermal drug delivery is limited by the extraordinary barrier properties of the stratum corneum (SC), the outer 10–15 μm layer of skin. Various approaches have therefore been proposed to increase the skin permeability such as through the following routes: chemical/lipid enhancers [7, 8], electric fields employing iontophoresis electroporation [9], electro-osmosis [10], pressure waves generated by ultrasound or photoacoustic effects [11, 12] and

radiofrequency (RF) thermal ablation [13]. More work, especially clinical studies, is needed to fully assess their potential impact [3, 14, 15].

During the last decades, microneedles fabricated using micro-electro-mechanical systems (MEMS) technology were developed as a novel and promising alternative for drug delivery. They provide a painless way to be easily inserted into skin to enhance the permeability of skin to drugs [5, 13, 15, 16]. The advantage of this method lies in that the injection causes no discomfort within the depths (20–100 μm) in the epidermis because the needles do not reach the upper end of the nerve cells. Meanwhile, the drug is however able to diffuse deeper into the skin and gets absorbed by the capillaries of the dermis and then enters the circulation system. Furthermore, such a system would be ideal for drugs that are not effective when taken orally either because of poor absorption or side effects such as induced liver damage [17]. Needles fabricated using MEMS technology can be classified into two major groups: in-plane needles where the needle shaft is fabricated in a plane parallel to the substrate [18] and out-of-plane needles, which have their shafts perpendicular to the wafer plane [3]. Over the past few years, a variety of different microneedle designs have been fabricated by employing techniques from the microelectronics industry and using materials such as silicon, metals, polymers and glass with feature sizes ranging from sub-micron to millimeters.

Although many microneedle designs have been available up to now, not all are capable of inserting into the skin. A variety of approaches have thus been taken to investigate their ability to inject drugs. Stoeber and Liepmann [17] made a single needle with sharp tip to deliver a fluorescent dye, Lucifer Yellow, into a chicken thigh. The pictures taken through confocal microscopy indicated that the fluid was successfully delivered more than 100 μm under the skin. Wang and his colleagues [19] monitored the penetration and infusion for single hollow microneedles from glass pipettes by a video microscopy. After the injection, the skin specimen was immediately immersed in liquid nitrogen and sectioned in a frozen microtome to a thickness of 7–12 μm . The puncture track, the depth and area of infused liquid were measured from the digitized image. The results showed that the loading depth ranged from 200 μm to 500 μm . The epidermis samples were also examined by scanning electron microscopy [15]. Because visual observation of needle insertion was extremely difficult, electrical resistance of the skin was also adopted to identify needle penetration [16]. To our best knowledge, no theoretical efforts had ever been made before to quantitatively predict the transient drug concentration distribution in the skin. To better understand the working performance of the microneedles, mathematical models were developed in this paper and numerical simulations were performed for describing kinetics of dispersed drug injected into skin from a microneedle array. In the following sections, the influence of the properties of the microneedle and tissue (such as the position of the microneedles tip, the cross section tip area of a single microneedle, the number of needles in the array, the injection velocity at the tip of the microneedle, tissue porosity and blood perfusion, etc) will be evaluated. Finally, some open questions, which await further investigations for improving the transdermal drug delivery, will be suggested.

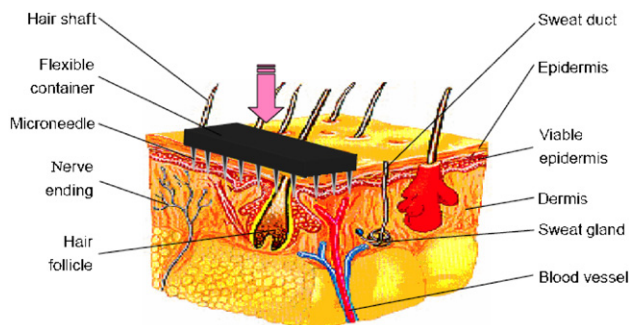


Figure 1. Schematic view of human skin and microneedle array.

2. Theoretical model

2.1. Tissue model and approximation

Physiologically, human skin is made up of three distinct layers: stratum corneum, viable epidermis and dermis [20]. The outer 10–15 μm layer of skin, called the stratum corneum, is primarily made of dead tissue. This layer is often the primary barrier for the external drug to overcome. The viable epidermis, up to 50–100 μm below the stratum corneum, contains living cells, but is devoid of blood vessels and contains few nerves. Deeper still, the dermis forms the bulk of skin volume and contains not only living cells, but also nerves and blood vessels. Injecting the drug just under the stratum corneum causes no pain however it is very effective for drug delivery, since the nerve endings appear deeper under the skin, and the presence of a large number of capillaries would help to absorb the drugs efficiently into the vascular system. A very typical concept for disposable microneedle arrays can be shown in figure 1. A deformable reservoir on the backside of an array of microneedles contains the drug solution. Merely pressing the device against the skin would deliver the medicine or vaccine. For easy handling and distributed delivery, some typical microneedles have been fabricated as large two-dimensional arrays perpendicular to the surface of the base material. Figure 2 gives some representative hollow microneedles fabricated from silicon, metal and glass [15, 16]. Once the compound runs across the stratum corneum, it will diffuse rapidly to the deeper tissue and be absorbed by the underlying capillaries.

For simplicity, the present theoretical model will be focused on the one-dimensional slab to simulate the drug transport along the skin depth during transdermal delivery with the microneedles (shown in figure 3). As is well known, biological systems are comprised of porous capillary bodies and cells that are heterogeneous, multi-phasic, and surface-dominated systems. It is reasonable to treat the skin tissue as a porous medium, which consists of solid particles and water [21]. The quantity of drug solution decreases along its flowing pathway due to absorption by the tissue cells, the inter-space of the tissue and the blood vessel. Here, we assume that the injected drug solution will be completely absorbed within a short period of time to take part in the cellular metabolism, and then returns to the venular blood. In the tissue, the ‘saturated tissues’ (defined as the region filled with injected drug solution) and the ‘unsaturated tissues’ are separated by

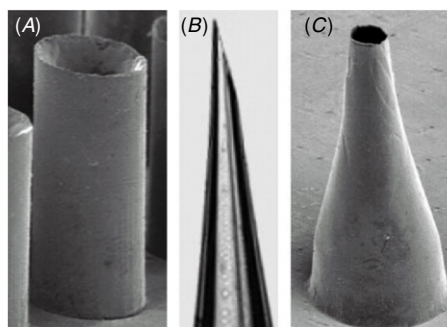


Figure 2. Hollow microneedles used for transdermal drug delivery, imaged by optical and scanning electron microscopy. (A) Straight-walled metal microneedle from a 100-needle array fabricated by electrodeposition on to a polymer mold (200 μm tall). (B) Tip of a tapered, beveled, glass microneedle made by a conventional micropipette puller (900 μm length shown). (C) Tapered hollow microneedle (500 μm tall) by electrodeposition of metal onto a polymeric mold [15, 16].

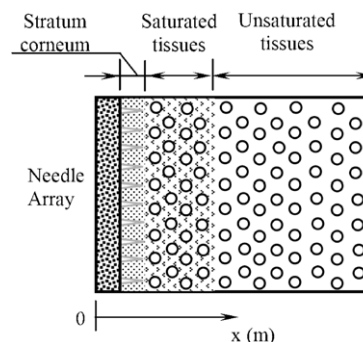


Figure 3. Model of drug delivery with a microneedle array.

a sharp moving interface. The moving interface advances along the x direction. To solve the problem, the following assumptions should be made:

- (1) A slab geometry is taken to represent the skin tissue and describe the transdermal drug delivery and transport across the porous media. Only the one-dimensional problem along the x direction is considered here for simplicity. The drug solution is assumed to be supplied with a constant velocity u_0 at the tip of microneedles during the injection process.
- (2) The properties of the skin tissue, the drug solution and the blood perfusion are assumed as uniform, neglecting their local variations.
- (3) The tissue is treated as a uniform porous medium, of which the specific vasculature is neglected in the model. In the tissue, ϵ_s is isotropic and independent of the normal direction and the position of any referenced section; thus, $\epsilon_s(x) = \epsilon_s$. Here, ϵ_s is defined as the areal porosity, which is the ratio of surface area occupied by drug solution to the whole surface area. This assumption then easily leads to $\epsilon_s = \epsilon_v = \epsilon$ [22], where ϵ is the general tissue porosity, and ϵ_v is defined as the volumetric porosity, which is the ratio of volume occupied by the drug solution to the total volume. If defining $S = A \cdot B$ as the surface area of the microneedle array (shown in figure 4), $\epsilon_s S$ represents the

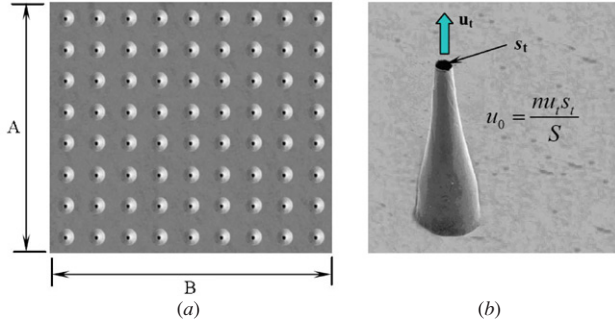


Figure 4. Schematic illustration for the effective injection velocity of the drug solution. (a) Sketch of the cross section of the microneedle array. (b) Relation between the effective injection velocity of the drug solution and a single microneedle (modified from [15, 16]).

effective area that drug solution can pass in tissue (treated as a homogenous porous medium).

- (4) The drug solution injected into the skin from the microneedles is assumed to be divided into three parts. The first part is absorbed by the tissue cells, with an absorption rate defined as α (m^3 drug solution/ m^3 tissue). The second part is taken away by blood vessels, which is proportional to the total volume. The proportion coefficient is expressed as β (m^3 drug solution/ m^3 tissue/s). The third part will fill the inter spaces of the tissue, which is also proportional to the total volume. The proportion coefficient is the volumetric porosity ε_v .
- (5) For the present needle injection case, the velocity with which the drug solution penetrates into the tissues is much larger than that for the drug species to diffuse away. That is to say, within a lamina space inside the moving interface of the drug solution, the solution is saturated any where at anytime. As is shown in figure 1, the microneedles are active systems by merely pressing the device against the skin. During the process of drug delivery, the velocity of drug solution plays a more important role than that of the diffusion at the boundary. This is because the concentration gradient there is very small and approximates to zero. Besides, the diffusion coefficient for the drug in skin is generally very small. Therefore, the position of the moving boundary does not depend on diffusion and hence can be decoupled from the system. This is a simple and intuitive approximation to make the solution feasible and useful.

2.2. Equations for characterizing the position of the moving interface

Once injected, the drug solution will gradually penetrate the tissue and be completely absorbed at a certain distal endpoint. The moving interface and its endpoint position depend on the injection velocity of the solution at the needle tip, as well as the diffusion and absorption properties of the tissues. Quantitative equations for characterizing this transient behavior will be established as follows. To calculate the moving interface, the volume $S(x_{\text{int}} - x_0)$ that the drug solution has passed through at time t is chosen as the

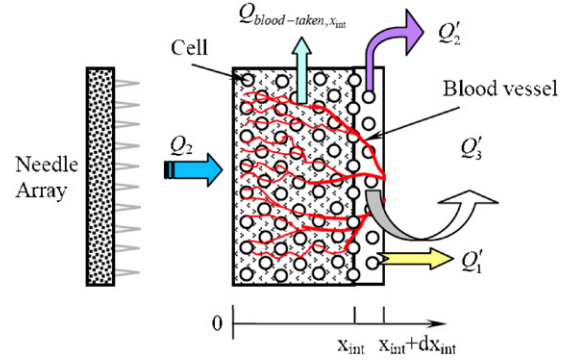


Figure 5. Mass conservation in a control volume.

control volume (shown in figure 5). Here, x_{int} represents the position of the moving interface at t , x_0 is the position of the microneedle tip. According to the assumptions made as above, the liquid injected into the skin from the microneedles over a time interval dt could be expressed as

$$Q_{\text{in}} = \varepsilon_s u_0 S \cdot dt, \quad (1)$$

where $u_0 = \frac{n u_i s_r}{S}$ is the effective injection velocity of drug solution which depends on the needle geometry and the number of needles in the array; u_i is the injection velocity of a single microneedle; $s_r = \pi d_{\text{needle}}^2 / 4$ is the cross section tip area of a single microneedle; d_{needle} is the diameter of the microneedle tip; n is the number of needles in the array.

In the control volume, the drug solution taken away by blood vessels in $x < x_{\text{int}}$ within dt is calculated as

$$Q_{\text{blood-taken}, x_{\text{int}}} = \beta \cdot S (x_{\text{int}} - x_0) dt. \quad (2)$$

Here, β represents the absorption coefficient of the drug taken away by blood vessels.

The moving interface will go forward a distance of dx_{int} within the time of dt . The drug solution loss, due to absorption by the interspaces of the tissue could then be defined as

$$Q'_1 = \varepsilon_v S \cdot dx_{\text{int}}. \quad (3)$$

Using the drug absorption rate for tissues α , the drug solution absorbed by the tissue cells in the lamina space dx_{int} reads as

$$Q'_2 = \alpha (1 - \varepsilon_v) S \cdot dx_{\text{int}}. \quad (4)$$

Simultaneously, the drug solution taken away by blood vessels in lamina space dx_{int} within dt could be evaluated as

$$Q'_3 = \beta \cdot V' \cdot dt = \beta \cdot S \cdot dx_{\text{int}} \cdot dt. \quad (5)$$

Owing to the continuous supplying of solution, there are no losses in this area due to absorption by the tissue or the inter-spaces. Therefore, based on the mass conservation in the control volume, a balance equation for the drug solution can be expressed as

$$Q_{\text{in}} = Q_{\text{blood-taken}, x_{\text{int}}} + Q'_1 + Q'_2 + Q'_3. \quad (6)$$

Substituting equations (1)–(5) into equation (6), one has

$$\varepsilon_s u_0 S \cdot dt = \beta \cdot S (x_{\text{int}} - x_0) \cdot dt + \varepsilon_v S \cdot dx_{\text{int}} + \alpha (1 - \varepsilon_v) S \cdot dx_{\text{int}} + \beta \cdot S \cdot dx_{\text{int}} \cdot dt. \quad (6a)$$

If the drug diffusion at the boundary is considered, an extra term related to $D_2 \frac{\partial C_2}{\partial x} M S dt / \rho$ will appear in the right-hand side of equation (6a) (here, D_2 is the drug diffusion coefficient

in skin; C_2 is the drug concentrations in skin tissue; ρ is the density of the drug solution (kg m^{-3}) and M is the weight of insulin per unit (kg/unit). This term is much less than other terms in the right-hand side of equation (6a) because the concentration gradient $\frac{\partial C_2}{\partial x}$ is very small and approximates to zero at the boundary and the drug diffusion coefficient in skin D_2 is generally very small.

Further, compared with other items, the fourth term on the right-hand side of the equation is a higher order infinitesimal, i.e. the differential term $dx_{\text{int}} \cdot dt$ is much smaller than a single dt or dx_{int} . Therefore, this term can be neglected without causing an evident error. Considering the assumption $\varepsilon_s = \varepsilon_v = \varepsilon$, equation (6a) can be simplified as

$$dt = \frac{\varepsilon + \alpha(1 - \varepsilon)}{\varepsilon u_0 - \beta(x_{\text{int}} - x_0)} dx_{\text{int}}. \quad (6b)$$

Integrating equation (6b) and substituting injector inlet condition $x_{\text{int}}|_{t=0} = x_0$ into it would easily yield the position of the moving interface as follows:

$$x_{\text{int}} = x_0 + \frac{u_0 \varepsilon}{\beta} \left[1 - e^{-\frac{\beta t}{\varepsilon + \alpha(1 - \varepsilon)}} \right]. \quad (7)$$

In this way, the transient position of the moving interface x_{int} at time t can be predicted. Further, if differentiating x_{int} by t using equation (7), the velocity for the moving interface can be obtained as

$$u_{\text{int}} = \frac{dx_{\text{int}}}{dt} = \frac{u_0 \varepsilon}{\varepsilon + \alpha(1 - \varepsilon)} \cdot e^{-\frac{\beta t}{\varepsilon + \alpha(1 - \varepsilon)}}. \quad (8)$$

When $t \rightarrow \infty$, the saturating position for the injected solution would reach its maximal value $x_{\text{int,max}}$, and the velocity of the moving interface approximates to zero $u_{\text{int}} \rightarrow 0$. Substituting this information into equation (7) leads to

$$x_{\text{int,max}} = x_0 + \frac{u_0 \varepsilon}{\beta}. \quad (9)$$

At this position, the liquid injected by the microneedles will be in equilibrium with the part taken away by the blood vessels.

2.3. Equation for characterizing the drug solution velocity

Different from deriving the moving front, another control volume $[x_0, x]$ is chosen to derive the velocity of the injected liquid transferring along the skin tissue. The drug solution taken away by blood vessels in this volume within time interval dt could be evaluated as

$$Q_{\text{blood-taken},x} = \beta \cdot S(x - x_0) \cdot dt \quad (10)$$

and the drug solution flows out of the control volume at position x is

$$Q_{\text{out},x} = \varepsilon_v u S \cdot dt. \quad (11)$$

Then using the mass-balance equation for drug solution in the control volume $[x_0, x]$, one has

$$Q_{\text{in}} = Q_{\text{blood-taken},x} + Q_{\text{out},x}. \quad (12)$$

After a combination of (1), (10), (11) and (12), the velocity for the drug solution u could easily be expressed as

$$u = u_0 - \frac{\beta(x - x_0)}{\varepsilon}. \quad (13)$$

2.4. Equation for characterizing the mass transport in skin tissue and the drug solution

In this section, we will derive the drug concentration distribution in the skin after its injection from the microneedle array. The subscripts 1 and 2 denote the drug and tissue, respectively. The mass-balance equation for the drug solution within the small control volume dx at position x could be stated as

$$\varepsilon u S = \varepsilon(u + du)S + \beta S \cdot dx. \quad (14)$$

Here, the term in the left-hand side gives the solution flowing into the control volume, while the right indicates the part escaping from the volume.

Further, applying the conservation law for the drug mass in this control volume, one can write out

$$\begin{aligned} \frac{\partial C_1}{\partial t} \varepsilon S \cdot dx &= u S \varepsilon C_1 - (u + du) S \varepsilon (C_1 + dC_1) - \beta C_1 S \cdot dx \\ &- D_1 \frac{\partial C_1}{\partial x} S \varepsilon + D_1 \left(\frac{\partial C_1}{\partial x} + \frac{\partial}{\partial x} \left(\frac{\partial C_1}{\partial x} \right) \cdot dx \right) S \varepsilon \\ &- \varphi (C_1 - C_2) S \cdot dx, \end{aligned} \quad (15)$$

where $\varphi (C_1 - C_2) S \cdot dx$ stands for the drug transport due to mass exchange between liquid and solid phase; C_1 is the drug concentrations in drug solution, respectively; D_1 is the diffusion coefficient in drug solution; and φ is the partition coefficient of the drug in skin tissue and can be defined as

$$\varphi = \frac{Sh D_2 A_0}{D'}. \quad (16)$$

This equation is proposed to calculate the partition coefficient of the drug in skin tissue in analogy to the volumetric heat convection coefficient between liquid and solid phases [23]. If the solid particle is approximated as having a spherical diameter d , then the specific area per unit volume of the tissue A_0 is equal to $6/d$. $D' = 4\varepsilon_v/A_0(1 - \varepsilon_v)$ represents the hydraulic diameter. For a forced convection over external boundaries in the presence of a porous medium, the Sherwood number Sh is approximately treated as $Sh = 2.0$ [24].

Substituting equation (14) into (15) reduces to

$$\frac{\partial C_1}{\partial t} + u \frac{\partial C_1}{\partial x} = D_1 \frac{\partial^2 C_1}{\partial x^2} - \frac{\varphi}{\varepsilon} (C_1 - C_2) - \frac{du}{dx} \frac{dC_1}{dx}. \quad (17a)$$

Here, the last term $\frac{du}{dx} \frac{dC_1}{dx}$ is a higher order infinitesimal one compared with any other terms in the equation, thus equation (17a) could be simplified as

$$\frac{\partial C_1}{\partial t} + u \frac{\partial C_1}{\partial x} = D_1 \frac{\partial^2 C_1}{\partial x^2} - \frac{\varphi}{\varepsilon} (C_1 - C_2). \quad (17b)$$

For the tissue phase in the porous medium, the mass-balance equation is similarly given as follows in analogy to the well-known Pennes' equation [25, 26] in which the blood perfusion term has been incorporated:

$$\begin{aligned} \frac{\partial C_2}{\partial t} (1 - \varepsilon) S \cdot dx &= -D_2 \frac{\partial C_2}{\partial x} (1 - \varepsilon) S \\ &+ D_2 \left(\frac{\partial C_2}{\partial x} + \frac{\partial}{\partial x} \left(\frac{\partial C_2}{\partial x} \right) \cdot dx \right) (1 - \varepsilon) S \\ &+ g S \cdot dx + \beta (C_1 - C_2) S \cdot dx + \varphi (C_1 - C_2) S \cdot dx, \end{aligned} \quad (18)$$

where g is the drug consumption rate per unit volume in tissue. In most time, the drug only releases either via enzymatic

Table 1. Parameters in the transport model.

Parameter	Value
Initial drug concentration C_0	100 units ml^{-1}
Diffusion coefficient in drug solution D_1	$5.0 \times 10^{-10} \text{ m}^2 \text{ s}^{-1}$
Diffusion coefficient in skin tissue D_2	$1.0 \times 10^{-10} \text{ m}^2 \text{ s}^{-1}$
Position of the microneedle tip x_0	15 μm [20, 29, 30]
Average porosity ε	0.2 [21, 22]
Drug solution absorption rate per unit tissue volume α	0.01 $\text{m}^3 \text{ drug solution}/\text{m}^3 \text{ tissues}$ [23]
Absorption coefficient β	0.005 $\text{m}^3 \text{ drug solution}/\text{m}^3 \text{ tissues} / \text{s}$ [21]
Initial effective injection velocity of drug solution u_0	$1.0 \times 10^{-5} \text{ m s}^{-1}$ [15]

activity or changes in physiological conditions such as pH, osmolality, or temperature once it was concentrated at the target. In the skin, g is always very small and approximates to zero. Equation (18) could be further simplified to

$$\frac{\partial C_2}{\partial t} = D_2 \frac{\partial^2 C_2}{\partial x^2} + \frac{g}{1-\varepsilon} + \frac{\beta + \varphi}{1-\varepsilon} (C_1 - C_2). \quad (19)$$

For the skin tissue area $x > x_{\text{int}}$ unsaturated by drug solution, the drug is transported through diffusion and blood perfusion. Then the governing equation for the drug concentration is established as follows:

$$\frac{\partial C_2}{\partial t} = D_2 \frac{\partial^2 C_2}{\partial x^2} - \frac{\beta C_2}{1-\varepsilon} + \frac{g}{1-\varepsilon}. \quad (20)$$

2.5. Initial and boundary conditions

As explained above, the fluid will gradually penetrate the tissue until become completely absorbed at some distal end point. The fundamental relations to be satisfied at such interface should reflect the facts that (a) there is no drug exchange in the liquid phase at the moving interface; (b) the continuity of drug concentration would exist at the moving interface in the tissue, and (c) a mass balance must be satisfied at the skin tissue. For the drug solution, the mass transfer by diffusion at the moving interface approximates to zero. Therefore, the boundary conditions at the moving interface take the following forms:

$$\frac{\partial C_1}{\partial x} = 0, \quad x = x_{\text{int}} \quad (21a)$$

$$\frac{\partial C_2}{\partial x} \Big|^- = \frac{\partial C_2}{\partial x} \Big|^+, \quad x = x_{\text{int}} \quad (21b)$$

$$C_2^- = C_2^+, \quad x = x_{\text{int}}. \quad (21c)$$

The boundary conditions for the whole calculation domain are defined as follows:

$$C_1 = C_2 = C_0, \quad x = x_0 \quad (22a)$$

$$\frac{\partial C_2}{\partial x} = 0, \quad x = L, \quad (22b)$$

where x_0 is the position of the microneedle tip. L is the length of the studied tissue.

Considering that at the beginning of the drug delivery, there is no drug distribution across the tissues, i.e. its concentration is zero. Therefore the initial conditions for the drugs in the skin and drug solution can be prescribed as follows:

$$C_1 = 0, \quad t = 0 \quad (23a)$$

$$C_2 = 0, \quad t = 0. \quad (23b)$$

In this paper, the standard finite difference method (FDM) is used to numerically solve the above series of coupling differential equations (13), (17a) and (20) with their continuity, initial and boundary conditions (21a)–(22b) together. In order to guarantee a high-resolution result and small oscillation in calculation, the well-known MacCormack's predictor–corrector iteration is particularly adopted to compile the FDM scheme. A similar computer program used to solve such a problem had been subjected to validation before in [21]. In addition, the results can also be compared with the experimental results [15].

2.6. Parameters of the transport model

In this study, typical cases via different injection speeds using the microneedle array filled with 100 units ml^{-1} ($C_0 = 100 \text{ units ml}^{-1}$) insulin (Humulin-R) will be calculated. The drug diffusivity in skin and drug solution is an important parameter affecting the drug delivery effect. Such data are currently not available in the published literature to our best knowledge. Nevertheless, they can still possibly be gathered from some previous work. For example, some solute diffusivities in dilute bulk solution within cylindrical holes have been determined by the following ways: calcein from the Stokes–Einstein equation [27] using molecular radius of 6.5 Å ($5.0 \times 10^{-6} \text{ cm}^2 \text{ s}^{-1}$), hexameric insulin from a semiempirical correlation ($1.3 \times 10^{-6} \text{ cm}^2 \text{ s}^{-1}$), BSA from experimental measurement [28] and viscosity by using the Stokes–Einstein equation ($5.9 \times 10^{-7} \text{ cm}^2 \text{ s}^{-1}$), and nanospheres by using the Stokes–Einstein equation ($1.3 \times 10^{-7} \text{ cm}^2 \text{ s}^{-1}$ and $6.5 \times 10^{-8} \text{ cm}^2 \text{ s}^{-1}$ for 25 nm and 50 nm radii, respectively). Here, without losing generality, the solute diffusivity in water and tissue are taken as $D_1 = 5.0 \times 10^{-10} \text{ m}^2 \text{ s}^{-1}$ and $D_2 = 1.0 \times 10^{-10} \text{ m}^2 \text{ s}^{-1}$, respectively. The injection is painless at the depths of 15 ~ 100 μm in the epidermis because the needles do not reach the upper nerve cells. The drug, however, is able to diffuse deeper into the skin and gets absorbed into the capillaries of the dermis. In this paper, the penetration depth is assumed as $x_0 = 15 \mu\text{m}$. This may represent the most disadvantageous case for drug delivery and a deeper depth could also be calculated by the same method. The typical values for the mass transfer properties of tissues and geometry for the microneedle tip are listed in table 1.

For brevity, only the insulin distribution in skin and drug solution will be given in this paper. However, the present approach can also possibly be extended to study a wider range

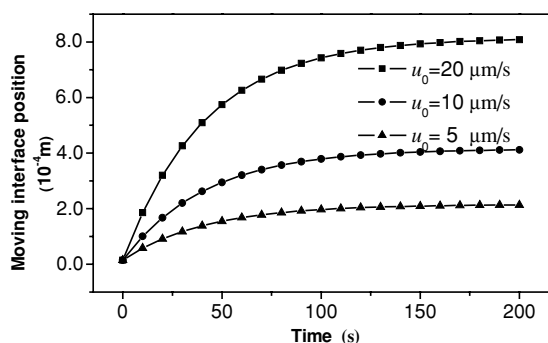


Figure 6. Influence of injection velocity on the position of the moving interface ($x_0 = 15 \mu\text{m}$, $\varepsilon = 0.2$, $\alpha = 0.01 \text{ m}^3 \text{ liquid/m}^3 \text{ tissue}$, $\beta = 0.005 \text{ m}^3 \text{ liquid/m}^3 \text{ tissue/s}$).

of drug species such as calcein, phosphate buffer saline (PBS) and other therapeutic agents.

3. Results and discussion

3.1. Moving interface

For convenience, the distance at which the moving interface of drug solution will reach its largest extent and is under the stagnant, was defined as ‘stagnant distance’. To some extent, such a ‘stagnant distance’ would reflect the performance of the microneedle, which is mainly dependent on the injection velocity u_0 , tissue porosities ε and blood absorption coefficient β . As is shown in figure 6, the moving interface will reach its largest extent $800 \mu\text{m}$ in about 200 s when the injection velocity is $20 \mu\text{m s}^{-1}$. Such a result qualitatively accords well with the experimental results conducted by McAllister *et al* [15]. There, they used single glass microneedle inserted into the skin of diabetic hairless rats *in vivo* to deliver insulin during a 30 min infusion. Their needles were fabricated using a micropipette puller and beveller with a tip radius of $60 \mu\text{m}$ and were inserted into the skin to a depth of $500\text{--}800 \mu\text{m}$. Through an analysis of their cases, the velocity of injection solution is near $20 \mu\text{m s}^{-1}$, just as used in our model. In the present numerical simulation, we had adopted almost equivalent parameters and the injection velocity as that treated in [15] for the transport model. Therefore, it can be reasonably accepted that the former experimental result has fairly validated the present theoretical predictions to some extent. But a complete comparison between experiment and theory is still not available at the present stage, due to the complexity of the problem itself. Further, it can also be found from figure 6 that the ‘stagnant distance’ decreases with a large gradient when the injection velocity decreases. It is noticed that the injection velocity strongly depends on the pressure applied on the deformable reservoir, which should not be very large in order to prevent the microneedles from fracture. The effects of microneedle tip geometry, injection/extraction pressure and time on the injected/extracted volume have been quantified with experiment by Wang and his colleagues [19].

Except for the injection velocity u_0 , the tissue property also influences the ‘stagnant distance’. Such a problem can easily be evaluated by the present theoretical model. As

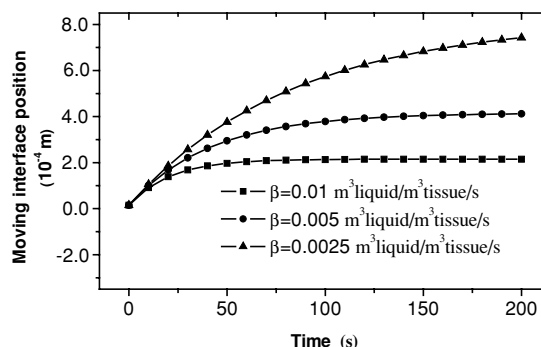


Figure 7. Influence of blood absorption coefficient on the position of the moving interface ($x_0 = 15 \mu\text{m}$, $\varepsilon = 0.2$, $u_0 = 1.0 \times 10^{-5} \text{ m s}^{-1}$, $\alpha = 0.01 \text{ m}^3 \text{ liquid/m}^3 \text{ tissue}$).

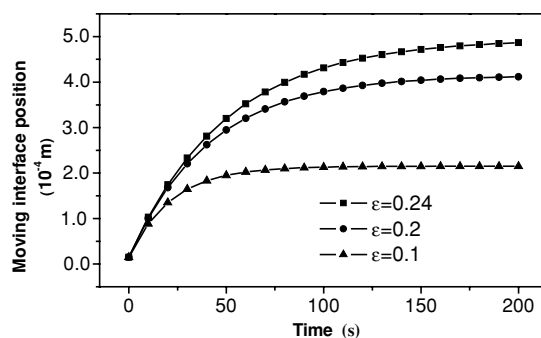


Figure 8. Influence of tissue porosities on the position of the moving interface ($x_0 = 15 \mu\text{m}$, $u_0 = 1.0 \times 10^{-5} \text{ m s}^{-1}$, $\alpha = 0.01 \text{ m}^3 \text{ liquid/m}^3 \text{ tissue}$, $\beta = 0.005 \text{ m}^3 \text{ liquid/m}^3 \text{ tissue/s}$).

indicated in figure 7, for the drug solution that will be absorbed by blood effects of the absorption coefficient β appears much evident. The drug solution could only reach a comparatively narrow range for a large value of β . On the other hand, it will reach a deeper area if less absorbed by blood. In many situations, the blood absorption coefficient β depends on the enzymatic activity or some physiological conditions such as pH, osmolality, or temperature. A targeted drug could increase the blood absorption coefficient and enhance the effect of the drug delivery with the microneedle array. Figure 8 gives the moving interface position of drug solution in tissue with different tissue porosities. It indicates that in the organ with a large porosity, allowing a high tissue specific permeability to drug solution, drug solution would infiltrate much easier and farther than that in the skin with a smaller porosity.

We also evaluate the effects of the fluid absorption rate per unit tissue volume α on the moving interface position. However, no evident differences were found among the moving interface positions under $\alpha = 0.02 \text{ m}^3 \text{ liquid/m}^3 \text{ tissue}$, $\alpha = 0.01 \text{ m}^3 \text{ liquid/m}^3 \text{ tissue}$ and $\alpha = 0.005 \text{ m}^3 \text{ liquid/m}^3 \text{ tissue}$, respectively. The result is thus omitted here. From the information as revealed in equations (7) and (9), one can find that α only affects the time for the moving interface to reach the ‘stagnant distance’, but not the ‘stagnant distance’ itself.

From the above analysis, it can be concluded that increasing the injection velocity and accelerating the blood

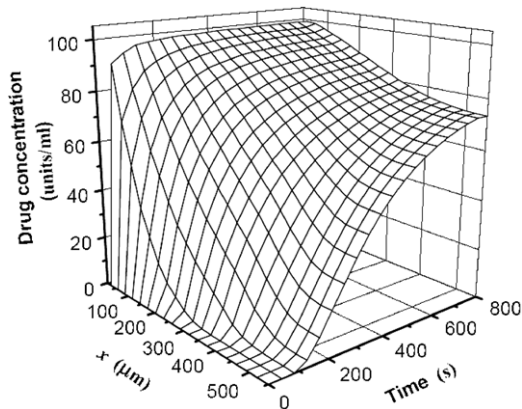


Figure 9. Transient distribution of drug concentration in the skin tissue ($x_0 = 15 \mu\text{m}$, $\varepsilon = 0.2$, $u_0 = 1.0 \times 10^{-5} \text{m s}^{-1}$, $\alpha = 0.01 \text{m}^3 \text{liquid/m}^3 \text{tissue}$, $\beta = 0.005 \text{m}^3 \text{liquid/m}^3 \text{tissue/s}$).

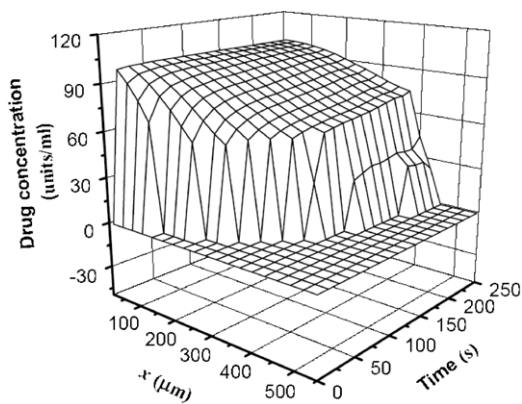


Figure 10. Transient and spatial distribution of drug concentration in the drug solution ($x_0 = 15 \mu\text{m}$, $\varepsilon = 0.2$, $u_0 = 1.0 \times 10^{-5} \text{m s}^{-1}$, $\alpha = 0.01 \text{m}^3 \text{liquid/m}^3 \text{tissue}$, $\beta = 0.005 \text{m}^3 \text{liquid/m}^3 \text{tissue/s}$).

circulation in high porosity skin tissue is helpful to enhance the transdermal drug delivery.

3.2. Transient drug concentration in tissue and solution

Further, in order to completely characterize the drug delivery with a microneedle, the drug concentrations in the skin tissue and drug solution are predicted and discussed. Figures 9 and 10 depict the transient drug concentration distribution across the skin tissue and drug solution, respectively. The largest drug concentration occurs at the microneedle tip and decreases gradually along the x direction in skin tissue and drug solution. For the case of $u_0 = 1.0 \times 10^{-5} \text{m s}^{-1}$, about 800 s is needed for the drug concentration in skin tissue to reach a steady state. However, a shorter time is needed under the same condition for the drug solution. The drug concentration in drug solution increased sharply as soon as it was injected into the skin. Figure 11 gives the steady state drug concentration versus distance in the drug solution and skin tissue, respectively. Clearly, the steady state drug concentration in the drug solution appears a little higher than that in the skin tissue within the area $x < x_{\text{int}}$. Beyond the moving interface, the drug could still penetrate a little far into the deep tissue through diffusion.

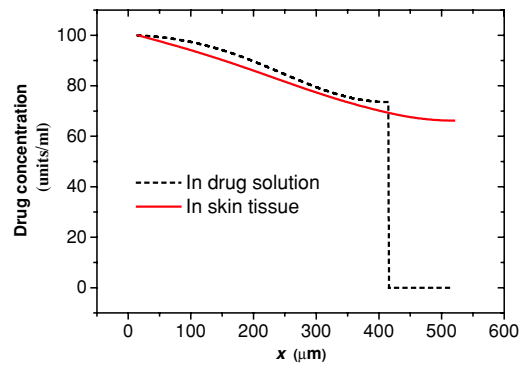


Figure 11. Steady state drug concentration distribution in the drug solution and skin tissue ($x_0 = 15 \mu\text{m}$, $\varepsilon = 0.2$, $u_0 = 1.0 \times 10^{-5} \text{m s}^{-1}$, $\alpha = 0.01 \text{m}^3 \text{liquid/m}^3 \text{tissue}$, $\beta = 0.005 \text{m}^3 \text{liquid/m}^3 \text{tissue/s}$).

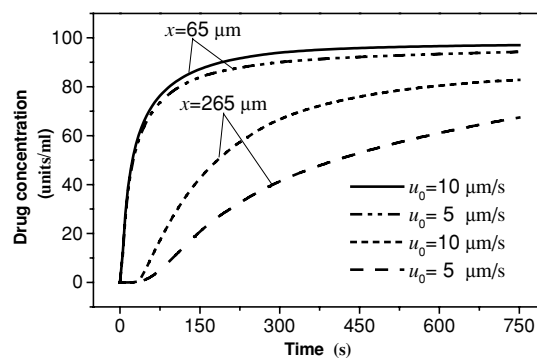


Figure 12. Influence of injection velocity on drug concentration in the skin tissue ($x_0 = 15 \mu\text{m}$, $\varepsilon = 0.2$, $\alpha = 0.01 \text{m}^3 \text{liquid/m}^3 \text{tissue}$, $\beta = 0.005 \text{m}^3 \text{liquid/m}^3 \text{tissue/s}$).

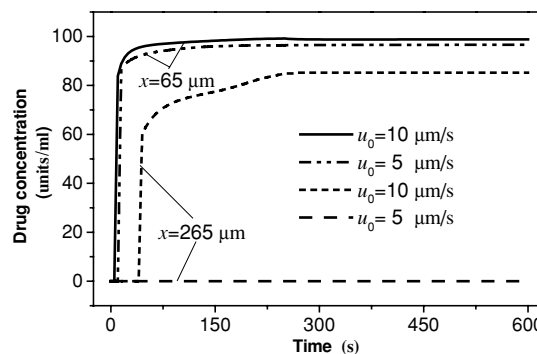


Figure 13. Influence of injection velocity on drug concentration in the drug solution ($x_0 = 15 \mu\text{m}$, $\varepsilon = 0.2$, $\alpha = 0.01 \text{m}^3 \text{liquid/m}^3 \text{tissue}$, $\beta = 0.005 \text{m}^3 \text{liquid/m}^3 \text{tissue/s}$).

3.2.1. Effect of initial injection velocity. To evaluate effects of the initial injection velocity u_0 , tissue porosities ε and blood absorption coefficient β on the drug concentration distribution and temporal response in both skin tissue and the drug solution, parametric analyses were given as follows.

Figures 12 and 13 reflect the influence of the initial injection velocity to the drug concentration in skin tissue and the drug solution, respectively. Obviously, for the pressure-driven flow, a higher injection velocity would increase the drug concentration over the skin tissue and the drug solution. In a steady state, the drug concentration decreases along the

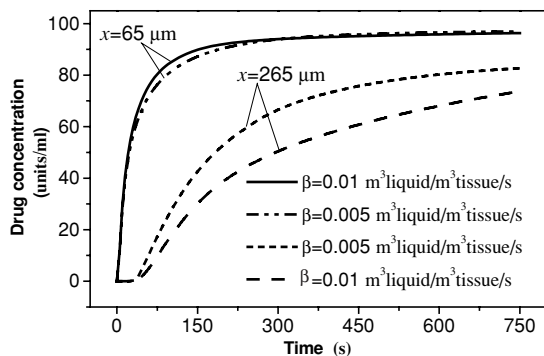


Figure 14. Influence of blood absorption coefficient on the drug concentration in the skin tissue ($x_0 = 15 \mu\text{m}$, $\varepsilon = 0.2$, $u_0 = 1.0 \times 10^{-5} \text{ m s}^{-1}$, $\alpha = 0.01 \text{ m}^3 \text{ liquid/m}^3 \text{ tissue}$).

x direction in the skin tissue and drug solution. At the beginning of injecting the drug solution with the microneedle, the drug concentration in the skin tissue far from the needle tip is close to zero because the moving interface has not reached there. For the case of a small injection velocity, the ‘stagnant distance’ is short and the drug concentration beyond this region appears very low. From this point, increasing the injection velocity is helpful to enhance the transdermal drug delivery. Clearly, increasing the velocity requires a large pressure applied on the microneedle. Exorbitant pressure may overcome the force limit that the microneedle can withstand and thus possibly makes it broken. Davis and his colleagues [16] have experimentally measured and theoretically modeled two critical mechanical events associated with microneedles: the force required to press microneedles into living skin and the force needles can withstand before fracturing. In order to enhance the transdermal drug delivery, increasing the injection velocity is a simple yet effective method, on condition that the needles could withstand the external force. Thus, more efforts are needed in the near future to optimize the material density, diameter and spacing of the microneedles.

3.2.2. Effect of blood absorption coefficient. Another approach to enhance the transdermal drug delivery is to strengthen the blood circulation. The presence of a large number of capillaries in the skin tissue helps to absorb the drug efficiently into the vascular system, which serves to deliver the drug to the whole body as it flows around. McAllister *et al* [15] collected the blood of diabetic hairless rats periodically by tail vein laceration and assayed for glucose concentration in blood. Their study demonstrated up to a 70% drop in blood glucose level over a 5-h period after the insulin was administered. Accelerating the blood circulation will enhance its role in delivering the drug. Figures 14 and 15 illustrate the influence of the blood absorption coefficient on the drug concentration in the skin tissue and drug solution, respectively. Clearly, the higher the blood absorption coefficient, the lower the drug concentration in the skin tissue and drug solution will be. On the contrary, the blood will bring more drugs away to other tissue sites far from the microneedles. Near the microneedle tip, the drug concentration distribution in the skin tissue and drug solution almost superpose together under different blood absorption coefficients. This indicates that the effect of the

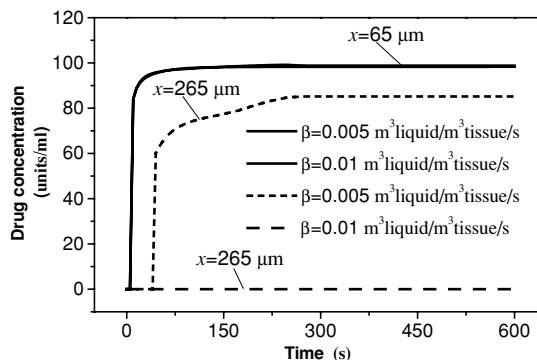


Figure 15. Influence of blood absorption coefficient on the drug concentration in the drug solution ($x_0 = 15 \mu\text{m}$, $\varepsilon = 0.2$, $u_0 = 1.0 \times 10^{-5} \text{ m s}^{-1}$, $\alpha = 0.01 \text{ m}^3 \text{ liquid/m}^3 \text{ tissue}$).

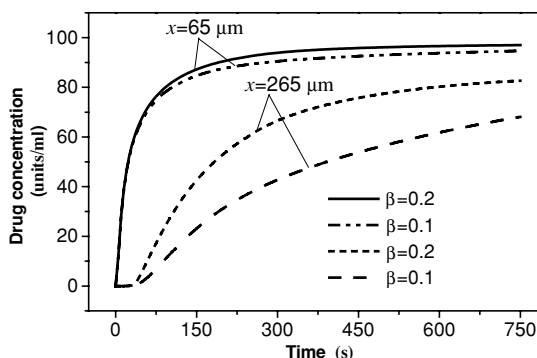


Figure 16. Influence of tissue porosities on the drug concentration in the skin tissue ($x_0 = 15 \mu\text{m}$, $u_0 = 1.0 \times 10^{-5} \text{ m s}^{-1}$, $\alpha = 0.01 \text{ m}^3 \text{ liquid/m}^3 \text{ tissue}$, $\beta = 0.005 \text{ m}^3 \text{ liquid/m}^3 \text{ tissue/s}$).

blood absorption coefficient on drug concentration gradually becomes weaker near the microneedle tip. The deeper the ‘stagnant distance’, the stronger the influence of the blood absorption coefficient to the drug concentration will be.

3.2.3. Effect of tissue porous media properties. Apart from the above two factors (the injection velocity u_0 and blood absorption coefficient β), the property of the skin tissue, such as the tissue porosities ε , also plays a key role in drug delivery. The drug concentration distribution in the skin tissue and drug solution with different tissue porosities due to injection is given in figures 16 and 17. It also indicates that in an organ with large porosity, representing a large tissue specific permeability to drug solution, the drug solution infiltrates much easier and farther than that in the skin with a smaller porosity.

3.3. Further routes to probe into the issue.

Clearly, what has been presented above still appears very preliminary. Tremendous efforts are needed to gain a more comprehensive understanding of the microneedle-based drug delivery process. Several fundamental issues especially worth of pursuing are as follows: (1) as was revealed, the presence of a large number of capillaries in the skin would help to absorb the drug efficiently into the vascular system. Besides, accelerating the blood circulation will enhance the delivery of the drug to the whole body. However, the maximal saturating

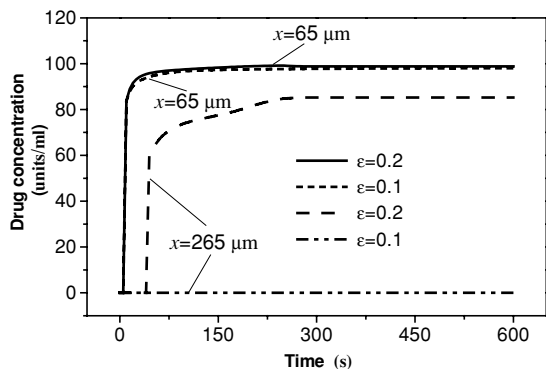


Figure 17. Influence of tissue porosities on the drug concentration in the drug solution ($x_0 = 15 \mu\text{m}$, $u_0 = 1.0 \times 10^{-5} \text{ m s}^{-1}$, $\alpha = 0.01 \text{ m}^3 \text{ liquid/m}^3 \text{ tissue}$, $\beta = 0.005 \text{ m}^3 \text{ liquid/m}^3 \text{ tissue/s}$).

distance is closely related to multiple variables such as x_0 , u_0 and ε , as well as β (seen in equation (9)). With the decrease of the blood absorption coefficient β , the position of the maximal saturating distance moves towards the body core. To realize a fairly large maximal saturating distance, the blood absorption coefficient β should not be too large. On the other hand, a large blood absorption coefficient β will help to take more drugs to the tissues far from the microneedles. Since there are more blood vessels in the deeper tissue, an optimum speed of blood circulation should be studied in advance (2). In addition, experimental measurements need to be performed to further quantify the present theoretical model (3). The position chosen for the injection should be the one with porosities ε as large as possible. Clearly, more experience is still needed for the clinicians and patients to appropriately operate the microneedle system (4). In some situations, blebs may be formed during the transdermal injections using small hypodermic needles. For such a case, a two-phase transport process will be involved, which needs further efforts in the near future.

4. Conclusion

This study provides the first quantitative modeling on the fluid injection kinetics through microneedle arrays and the drug species transport across the skin. The effects of the properties of the microneedles and tissues such as needle tip size, the solution injection velocity at the tip of the needles, the tissue porosity and the blood perfusion rate, etc., to the transdermal drug delivery processes were comprehensively investigated through numerical calculation. It can be found that increasing the injection velocity and accelerating the blood circulation in skin tissue will help enhance the drug delivery to some extent, which offers certain practical ways for better administrating the operation of the microneedle array. The modeling approach as suggested in this paper can possibly be extended to a wider range of transport issues such as targeted nano-particle delivery for therapeutics or molecular imaging. Considering that dynamically measuring *in vivo* the drug species concentration in an extremely small tissue area requires a highly sophisticated apparatus and is generally rather difficult, if not impossible, the present theoretical prediction provides an alternative way to better understand

the complete picture of the drug delivery process enabled by microneedles. Further efforts can be made along this direction in the near future by taking into account more specific considerations. Clearly, probing into such issues will help push forward the progress of microneedle-based drug delivery technology.

Acknowledgments

This work was supported by the National Natural Science Foundation of China under grants 50575219 and 50325622.

References

- [1] Park K 1997 *Controlled Drug Delivery: Challenges and Strategies* (Washington, DC: American Chemical Society) pp 54–80
- [2] Langer R 1998 *Nature* **392** 5
- [3] Henry S, McAllister D V, Allen M G and Prausnitz M R 1998 *J. Pharm. Sci.* **87** 922
- [4] Langer R 1990 *Science* **249** 1527
- [5] Prausnitz M R 2004 *Adv. Drug Deliv. Rev.* **56** 581
- [6] Bronaugh R L and Maibach H I 1999 *Percutaneous Absorption: Drugs–Cosmetics–Mechanisms–Methodology* (New York: Dekker)
- [7] Barry B and Williams A 2004 *Adv. Drug Deliv. Rev.* **56** 603
- [8] Cevc G 2004 *Adv. Drug Deliv. Rev.* **56** 675
- [9] Preat V and Vanbever R 2004 *Adv. Drug Deliv. Rev.* **56** 659
- [10] Pikal M J 2001 *Adv. Drug Deliv. Rev.* **46** 281
- [11] Doukas A 2004 *Adv. Drug Deliv. Rev.* **56** 559
- [12] Mitragotri S and Kost J 2004 *Adv. Drug Deliv. Rev.* **56** 589
- [13] Sintov A C, Krymberk I, Daniel D, Hannan T and Sohn Z 2003 *J. Control. Release* **89** 311
- [14] Prausnitz M R, Mitragotri S and Langer R 2004 *Nat. Rev. Drug Discov.* **3** 115
- [15] McAllister D V, Wang P M, Davis S P, Park J H, Canatella P J, Allen M G and Prausnitz M R 2003 *Proc. Natl Acad. Sci.* **100** 13755
- [16] Davis S P, Landis B J, Adams Z H, Allen M G and Prausnitz M R 2004 *J. Biomech.* **37** 1155
- [17] Stoeber B and Liepmann D 2000 *1st Ann. Int. IEEE-EMBS Special Topic Conf. on Microtechnologies in Medicine and Biology (October, Lyon, France)* pp 224–8
- [18] Leboutz K S and Pisano A P 1998 *Proc. Symp. Microstructures and Microfabricated Systems IV (Boston, MA, 1–6 November 1998)* (Pennington, NJ: Electrochemical Society) pp 235–44
- [19] Wang P M, Cornwell M G and Prausnitz M R 2002 *Proc. Second Joint EMBS/BMES Conf. (October, Houston, TX, USA)* vol 1 pp 506–7
- [20] Champion R H, Burton J L and Ebling F J G 1992 *Textbook of Dermatology* (London: Blackwell Scientific)
- [21] Gui L and Liu J 2005 *Heat Transfer Eng.* **26** 73
- [22] Bejan A 1999 *Convection in Porous Media* (New York: Springer)
- [23] Tien C L and Vafai K 1989 *Adv. Appl. Mech.* **27** 225
- [24] Manca D and Rovaglio M 2003 *Chem. Eng. Sci.* **58** 1337
- [25] Pennes H H 1948 *J. Appl. Physiol.* **1** 93
- [26] Liu J 2004 *ASME Int. Mechanical Engineering Congress and RD&D Expo (Anaheim, California, 13–20 November 2004)* pp 1–10
- [27] Poling B E, Prausnitz J M and O'Connell J P 2001 *The Properties of Gases and Liquids* (New York: McGraw-Hill)
- [28] Tyn M T, Gusek T W, Canatella J P, Allen M G and Prausnitz M R 1990 *Biotech. Bioeng.* **35** 327
- [29] Liu J and Wang C 1997 *Bioheat Transfer* (Beijing: Science Press) pp 102–29 (in Chinese)
- [30] Torvi D A and Dale J D 1994 *ASME J. Biomech. Eng.* **116** 250